Journal of Applied Mechanics and Technical Physics, Vol. 48, No. 2, pp. 250–259, 2007

VISCOPLASTIC DYNAMICS OF ISOTROPIC PLATES OF VARIABLE THICKNESS UNDER EXPLOSIVE LOADING

Yu. V. Nemirovskii and A. P. Yankovskii

UDC 539.4

A problem of viscoplastic dynamic bending of isotropic plates of variable thickness is formulated. A method for integrating the initial-boundary problem is developed. Numerical results are compared with a known analytical solution obtained within a rigid-plastic model; good agreement is demonstrated. The efficiency of the method developed is verified by numerical computations. It is shown that the final flexure of plates can be reduced severalfold by applying rational design.

Key words: *plates, explosive loading, inelastic dynamics, viscoplastic deformation, rational design.*

Introduction. Small and large plates form the basis of numerous protective fences and elements in shipbuilding, machine-building, and aviation engineering, as well as in construction industry. Under high-intensity dynamic loading, the damage of these elements largely determines the possibility of subsequent operation of these objects. The problem of dynamic calculation of such structural elements, therefore, is one of the most important problems in mechanics of deformable solids. The majority of the currently existing solutions are based on the model of an ideal rigid-plastic solid (see [1, 2] and other publications). The solutions are normally approximate and are obtained with the use of extreme principles of dynamics of a rigid-plastic body [3]. The solutions have been constructed for uniform isotropic plates of constant thickness, the dependence of the yield stress of the plate material on the strain rate being ignored. It is known, however, that rational definition of the plate thickness can exert a significant effect on plate resistance (in particular, dynamic resistance) to external forcing, and the dependence of the yield stress (e.g., for steels [4]) on the strain rate may be fairly significant and cannot fail to affect deformation of a thin-walled structure under dynamic loading. In particular, the neglect of this circumstance is one of the reasons for overprediction of the final flexure by 30 to 80% [2] in numerical calculations over experimental data.

The present study was aimed at developing a method for solving the initial-boundary problem of dynamic viscoplastic bending of isotropic plates of constant and variable thickness with allowance for viscoplastic hardening of the plate material and at analyzing the influence of the plate contour on the magnitude of the final flexure under explosive loading.

1. Formulation of the Problem. We consider transverse dynamic bending of a plate of variable thickness H. We introduce an orthogonal (possibly, curvilinear) coordinate system (x_1, x_2, z) such that the plane $z = 0$ coincides with the mid-plane of the plate before deformation begins. The transverse distributed load $p(x_1, x_2, t)$ acts in the z direction; in the case of small flexure w, therefore, the equation of motion of such a plate has the form [5]

$$[M_{11,1} + fM_{12,2} + \beta(M_{11} - M_{22})/x_1]_{,1} + f(M_{12,1} + fM_{22,2} + 2\beta M_{12}/x_1)_{,2}$$

$$+ \beta[M_{11,1} + fM_{12,2} + \beta(M_{11} - M_{22})/x_1]/x_1 + p(\boldsymbol{x}, t) = \rho H(\boldsymbol{x}) w(\boldsymbol{x}, t)_{,tt}. \quad (1)$$

Khristianovich Institute of Theoretical and Applied Mechanics, Siberian Division, Russian Academy of Sciences, Novosibirsk 630090; nemirov@itam.nsc.ru. Translated from Prikladnaya Mekhanika i Tekhnicheskaya Fizika, Vol. 48, No. 2, pp. 123–134, March–April, 2007. Original article submitted April 6, 2006.

Here

$$f = \begin{cases} 1, & \beta = 0, \\ 1/x_1, & \beta = 1 \end{cases} \tag{2}$$

[$\beta = 0$ if (x_1, x_2, z) is a Cartesian coordinate system and $\beta = 1$ if (x_1, x_2, z) is a cylindrical coordinate system],

$$M_{ij}(\boldsymbol{x}, t) = \int\limits_{-H/2}^{H/2} \sigma_{ij}(\boldsymbol{x}, z, t) z \, dz, \qquad i, j = 1, 2, \quad \boldsymbol{x} = \{x_1, x_2\} \in G, \tag{3}$$

M_{ij} are the moments arising in the plate, σ_{ij} is the stress in the structure, ρ is the bulk density of the material, G is the projection of the region occupied by the plate onto the plane $z = 0$; if a cylindrical polar coordinate system is used, x_1 is the polar radius and x_2 is the polar angle; the subscripts after the comma indicate partial differentiation with respect to the spatial variables x_1 and x_2 or with respect to time t.

According to the viscoplastic model [6], the stress σ in a uniaxial stressed state depends on the strain rate ξ of the material. Approximating the dependence $\sigma \sim \xi$ by a two-segment broken line (other approximations are also possible, e.g., a multi-segment broken line), we obtain

$$\sigma = \begin{cases} E\xi, & |\xi| \leqslant \xi_s = \sigma_s / E, \\ \text{sign } (\xi)\sigma_s + E_s(\xi - \text{sign } (\xi)\xi_s), & |\xi| > \xi_s, \end{cases} \tag{4}$$

where E and E_s are the coefficients of linear viscosity and linearly viscous hardening of the material, σ_s is the stress at the hinge point of the two-segment broken line approximating the dependence $\sigma \sim \xi$ (σ_s can be interpreted as the yield stress of the material). We reach a limiting transition to the rigid-viscoplastic model as $E \to \infty$ and to the rigid-plastic model at $E_s = 0$ and $E \to \infty$.

The plate behavior obeys Kirchhoff's laws; hence, in the case of small flexure, the strain ε_{ij}, the strain rate ξ_{ij}, the flexure w, and the flexure rate v are related as follows [5, 6]:

$$\varepsilon_{ij}(\boldsymbol{x}, z, t) = z\varkappa_{ij}(\boldsymbol{x}, t), \qquad \xi_{ij}(\boldsymbol{x}, z, t) = z\dot{\varkappa}_{ij}(\boldsymbol{x}, t), \qquad i, j = 1, 2, \quad |z| \leqslant H(\boldsymbol{x})/2. \tag{5}$$

Here

$$\dot{\varkappa}_{11} = -v_{,11}, \qquad \dot{\varkappa}_{22} = -f^2 v_{,22} - \beta v_{,1}/x_1, \qquad \dot{\varkappa}_{12} = \dot{\varkappa}_{21} = -f v_{,12} + \beta v_{,2}/x_1^2; \tag{6}$$

the expressions for the parameters of bending of the plate mid-plane $\varkappa_{ij}$ are obtained from Eq. (6) with v replaced by w; the dot indicates the derivative with respect to time.

Using relations (3)–(5) and the governing equations for materials with nonlinear viscosity [6], we obtain the moments M_{ij} in the form

$$M_{ii} = C_{iiii}\dot{\varkappa}_{ii} + C_{iijj}\dot{\varkappa}_{jj}, \qquad M_{ij} = 2C_{ijij}\dot{\varkappa}_{ij}, \qquad j = 3 - i, \quad i = 1, 2, \tag{7}$$

where the expressions for the coefficients C_{ijkl} depend nonlinearly on H and $\dot{\varkappa}_{mn}$ and are rather cumbersome. By virtue of the known formal similarity of the governing equations of the theory of elastoplastic deformation and the theory of viscoplastic flow [7], the expressions for C_{ijkl} coincide with the expressions for similar coefficients obtained in [8] for elastoplastic bending of plates with linear hardening (in this case, one should set $\nu = 1/2$ and $\omega_k = 0$ $(1 \leqslant k \leqslant N)$ in [8] and replace $-w_{,mn}$ by $\dot{\varkappa}_{mn}$; in the case of axisymmetric bending of a circular plate, the coefficients C_{ijkl} at $E_s = 0$ were determined in [9]).

With allowance for Eq. (6), we substitute the expressions for the moments (7) into the equation of motion (1) and write the latter (for convenience of further discussion) as a system of two equations

$$\rho H(\boldsymbol{x})v_{,t} = p(\boldsymbol{x}, t) - D(v), \qquad w_{,t} = v(\boldsymbol{x}, t) \qquad (t \geqslant 0, \quad \boldsymbol{x} \in G), \tag{8}$$

where

$$D(v) = \{[C_{1111}v_{,11} + C_{1122}(f^2 v_{,22} + \beta v_{,1}/x_1)]_{,1} + 2f[C_{1212}(f v_{,12} - \beta v_{,2}/x_1^2)]_{,2}$$

$$+ \beta(C_{1111} - C_{1122})(v_{,11} - f^2 v_{,22} - \beta v_{,1}/x_1)/x_1\}_{,1} + f\{2[C_{1212}(f v_{,12} - \beta v_{,2}/x_1^2)]_{,1}$$

$$+ f[C_{1122}v_{,11} + C_{1111}(f^2 v_{,22} + \beta v_{,1}/x_1)]_{,2} + 4\beta C_{1212}(f v_{,12} - \beta v_{,2}/x_1^2)/x_1\}_{,2}$$

$$+\beta\{[C_{1111}v_{,11}+C_{1122}(f^2v_{,22}+\beta v_{,1}/x_1)]_{,1}+2f[C_{1212}(fv_{,12}-\beta v_{,2}/x_1^2)]_{,2}$$

$$+\beta(C_{1111}-C_{1122})(v_{,11}-f^2v_{,22}-\beta v_{,1}/x_1)/x_1\}/x_1. \tag{9}$$

For simultaneous integration of system (8), we have to use the initial conditions

$$w(\boldsymbol{x},t_0)=w_0(\boldsymbol{x}),\qquad v(\boldsymbol{x},t_0)=v_0(\boldsymbol{x}) \tag{10}$$

and the known boundary conditions [5], which are not given here. [If kinematic boundary conditions are set for the flexure w, the second equality in (8) can be used to obtain the corresponding conditions for the flexure rate v. If static boundary conditions are set on the edges, relations (6) and (7) should be used.]

2. Method for Solving the Initial-Boundary Problem. If the rate v is known, the flexure w can be readily determined from the second equation in (8) under the first initial condition of (10). The first equation in (8) is a parabolic-type quasi-linear partial differential equation closed with respect to the flexure rate v, which contains the first-order derivative of v with respect to time t and up to the fourth-order derivatives with respect to the variables x_1 and x_2.

For numerical integration with respect to time t of the initial-boundary problem corresponding to the first equation in (8), we use one of the generalized Runge–Kutta methods, namely, the two-stage generalized Lobatto method IIIA (method of trapezoids) (see [10]), which has the second-order accuracy with respect to τ (τ is the step in time t). According to this method, we obtain

$$v^{n+1}(\boldsymbol{x})=v^n(\boldsymbol{x})+\tau(p^n(\boldsymbol{x})-D(v^n(\boldsymbol{x}))+p^{n+1}(\boldsymbol{x})-D(v^{n+1}(\boldsymbol{x})))/(2\rho H(\boldsymbol{x})), \tag{11}$$

where

$$p^n(\boldsymbol{x})=p(\boldsymbol{x},t_n),\qquad v^n(\boldsymbol{x})=v(\boldsymbol{x},t_n),\qquad t_{n+1}=t_n+\tau,\quad n=0,1,2,\ldots\quad (t_0=0), \tag{12}$$

the time step $\tau>0$ may be variable ($\tau=\tau_n$).

We write Eq. (11) in the form

$$\tau D(v^{n+1})+2\rho H(\boldsymbol{x})v^{n+1}=2\rho H(\boldsymbol{x})v^n+\tau(p^n(\boldsymbol{x})+p^{n+1}(\boldsymbol{x}))-\tau D(v^n). \tag{13}$$

If the flexure rate v^n at the nth time step is known, Eq. (13) with allowance for Eq. (9) determines the solution at the next $(n+1)$th layer. The drawback of Eq. (13) is the necessity of applying a nonlinear differential operator D to the known function v^n to calculate the right side of this equation. To avoid differentiation in the right side of Eq. (13), we consider the functions

$$P_n(\boldsymbol{x})=\tau D(v^n(\boldsymbol{x}))+2\rho H(\boldsymbol{x})v^n(\boldsymbol{x}),\qquad n=0,1,2,\ldots\ . \tag{14}$$

Then, the resolving Eq. (13) acquires the form

$$\tau D(v^{n+1}(\boldsymbol{x}))+2\rho H(\boldsymbol{x})v^{n+1}(\boldsymbol{x})=P_{n+1}(\boldsymbol{x}), \tag{15}$$

where the right side is known and is found from the recurrent formula

$$P_{n+1}(\boldsymbol{x})=-P_n(\boldsymbol{x})+4\rho H(\boldsymbol{x})v^n(\boldsymbol{x})+\tau(p^n(\boldsymbol{x})+p^{n+1}(\boldsymbol{x})) \tag{16}$$

obtained by comparing Eq. (14) and the right side of Eq. (13).

For zero initial conditions [see Eq. (10)]

$$v^0(\boldsymbol{x})=v_0(\boldsymbol{x})=0, \tag{17}$$

Eq. (14) with allowance for Eq. (9) yields

$$P_0(\boldsymbol{x})=0, \tag{18}$$

and Eqs. (16)–(18) yield

$$P_1(\boldsymbol{x})=\tau(p^0(\boldsymbol{x})+p^1(\boldsymbol{x})). \tag{19}$$

Thus, for determining the flexure rate at the $(n+1)$th time step, we have to integrate Eq. (15) with the known right side (16) [with allowance for Eqs. (17)–(19)] under appropriate boundary conditions obtained from the boundary conditions for the first equation in (8) by formal replacement of v by v^{n+1}.

Equation (15) with allowance for Eq. (9) is a fourth-order quasi-linear elliptic equation, and it can be interpreted as an equation of equilibrium of steady-state creep of a transversely bent plate on a linearly viscous base. By virtue of the formal similarity of equations of steady-state creep (within the framework of the flow theory) and equations of the theory of elastoplastic deformations [7], equality (15) coincides with the equation of static elastoplastic transverse bending of a plate on a linearly elastic base, if the function v^{n+1} is understood as flexure. The boundary-value problem corresponding to Eq. (15) can be integrated, therefore, by known methods of statics or steady-state creep.

Equation (15) can be linearized by an iterative method proposed in [7] for solving problems of steady-state creep, which is similar to the method of variable parameters of elasticity, widely used in solving elastoplastic problems in statics [11]. The method of variable parameters of elasticity was adapted to plates subjected to bending in [8]. After such linearization, Eq. (15) can be considered as a linear elliptic equation of bending of an isotropic inhomogeneous plate on a linearly elastic base and can be integrated with the use of numerical, variational, and other methods, which have been well developed in the theory of bent plates [12]. (The convergence of the method of variable parameters of elasticity was proved in [9, 11].)

As the initial approximation $v^m_{(0)}(\boldsymbol{x})$ for the function $v^m(\boldsymbol{x})$, we can use the solution at the previous time layer

$$v^m_{(0)}(\boldsymbol{x}) = v^n(\boldsymbol{x}), \qquad m = n+1$$

or the function

$$v^m_{(0)}(\boldsymbol{x}) = 3v^n(\boldsymbol{x}) + (\tau p^n(\boldsymbol{x}) - P_n(\boldsymbol{x}))/(\rho H(\boldsymbol{x})) \qquad (m = n+1)$$

obtained by Taylor's formula $v^m(\boldsymbol{x}) = v^n(\boldsymbol{x}) + \tau v_{,t}\,(\boldsymbol{x}, t_n) + O(\tau^2)$ with allowance for the expression for $v_{,t}$ from (8) and the operator $D(v^n)$ from (14) under the assumption that the solution of the problem at the previous nth time layer is known.

Let us consider a model problem of axisymmetric dynamics of circular and ring-shaped plates of variable thickness along the radius r. The load p, the manner of plate attachment, and the plate thickness are assumed to be independent of the polar angle x_2; hence, the flexure and its rate are also independent of x_2. In this case, Eq. (15) with allowance for Eq. (9) can be reasonably written as a system of two ordinary differential equations with respect to $M^m_r(r)$ and $v^m(r)$ $(r \equiv x_1)$:

$$\begin{gathered} -\tau\,\frac{d^2M^m_r}{dr^2} + A_1\,\frac{dM^m_r}{dr} - A_2M^m_r - B_1\,\frac{d^2v^m}{dr^2} - B_2\,\frac{dv^m}{dr} + 2\rho H(r)v^m = P_m(r), \\ -M^m_r - C_{1111}\,\frac{d^2v^m}{dr^2} - \frac{C_{1122}}{r}\,\frac{dv^m}{dr} = 0, \qquad m = n+1, \quad r_0 < r < r_1. \end{gathered} \tag{20}$$

In these equations,

$$\begin{gathered} A_1 = -\frac{\tau}{r}\,(2-a), \qquad A_2 = -\frac{\tau}{r}\,\frac{da}{dr}, \qquad B_1 = -\frac{\tau b}{r}, \qquad B_2 = -\frac{\tau}{r}\,\frac{db}{dr}, \\ a = C_{1122}/C_{1111}, \qquad b = (C^2_{1122}/C_{1111} - C_{2222})/r; \end{gathered} \tag{21}$$

$M^m_r(r) \equiv M^m_{11}(r)$ is the radial moment in the plate at the mth time layer, r_0 and r_1 are the radii of the inner and outer $(0 < r_0 < r_1)$ edges of the plate, and the function $P_m(r)$ is determined by Eq. (16) with $\boldsymbol{x}$ replaced by r.

We linearize system (20) by the method indicated above. Let $v^m_{(k)}(r)$ and $M^m_{(k)}(r)$ be known kth approximations of the sought functions v^m and M^m_r. Then, the next approximations of these functions can be determined by the system of linear equations

$$\begin{gathered} -\tau\,\frac{d^2M^m_{(l)}}{dr^2} + A^{(k)}_1\,\frac{dM^m_{(l)}}{dr} - A^{(k)}_2M^m_{(l)} - B^{(k)}_1\,\frac{d^2v^m_{(l)}}{dr^2} - B^{(k)}_2\,\frac{dv^m_{(l)}}{dr} + 2\rho H v^m_{(l)} = P_m, \\ -M^m_{(l)} - C^{(k)}_{1111}\,\frac{d^2v^m_{(l)}}{dr^2} - \frac{C^{(k)}_{1122}}{r}\,\frac{dv^m_{(l)}}{dr} = 0, \qquad m = n+1, \quad l = k+1, \quad r_0 < r < r_1, \end{gathered} \tag{22}$$

where the coefficients $A^{(k)}_i$ and $B^{(k)}_i$ $(i = 1, 2)$ are known and are found from Eqs. (21) with the use of the function $v^m_{(k)}$ (see [8]).

System (22) should be subjected to boundary conditions. At the center of a circular plate, we have

$$\frac{dv_{(l)}^m}{dr} = 0, \qquad \frac{dM_{(l)}^m}{dr} = 0, \qquad m = n+1, \quad l = k+1, \quad r = 0. \tag{23}$$

The conditions on the plate edges are

$$v_{(l)}^m = 0, \quad M_{(l)}^m = 0, \quad m = n+1, \quad l = k+1 \quad \text{for} \quad r = r_0 \quad \text{and} \quad r = r_1 \tag{24}$$

if the plate is simply supported and

$$v_{(l)}^m = 0, \quad \frac{dv_{(l)}^m}{dr} = 0, \quad m = n+1, \quad l = k+1 \quad \text{for} \quad r = r_0 \quad \text{and} \quad r = r_1 \tag{25}$$

if the plate is clamped. (Other support conditions can also be imposed, e.g., support conditions on a viscoelastic base, etc.)

Replacing the derivatives in Eqs. (22), (23), and (25) by finite differences on a uniform grid along r with a step h, we obtain finite-difference analogs of Eqs. (22) and boundary conditions (23) and (25) with the second order of approximation in terms of h for a three-point template. To solve the corresponding system of linear algebraic equations, we can use a stable matrix sweep method [13].

Numerous calculations show that the iterative process (22)–(25) always converges.

If the flexure rate at the nth and $(n+1)$th time layers is known, we can use the second equation in (8) and the method of trapezoids [with allowance for the first initial condition in (10)] to determine the flexure at the $(n+1)$th layer with the second-order accuracy in terms of τ:

$$w^{n+1} = w^n + \tau(v^n + v^{n+1})/2, \qquad n = 0, 1, 2, \ldots \ . \tag{26}$$

In the case of viscoplastic deformation, the resolving equation of plate dynamics [the first equation in (8) with allowance for (9)] is a parabolic-type quasi-linear equation with respect to the flexure rate v. It is known that the general theory of stability and convergence of finite-difference schemes has not been adequately developed for quasi-linear differential equations [14]. Therefore, the basic criterion of reliability of any finite-difference scheme is based on approximate solutions of test (model) problems whose analytical solutions are known.

The authors have not yet proved the stability of the numerical scheme (15), (26) in the general case, where the operator D [see Eq. (9)] is nonlinear. Nevertheless, the stability of this scheme is supported by the physical correctness (noncontradiction) of results of numerous calculations and the good agreement between numerical results and available analytical solutions (see Sec. 3). In the case of linear viscosity [see Eq. (4) with $\xi_s \to \infty$], the spectral stability of scheme (13), (15) can be proved by repeating all reasoning in [10] used to prove the stability of the generalized Runge–Kutta methods for solving the problem of unsteady heat conduction, which is described by a parabolic equation containing a derivative with respect to time t of the first order only [like the first equation in (8)].

3. Discussion of Calculated Results on Inelastic Dynamics of Circular and Ring-Shaped Plates. Let us examine dynamic viscoplastic bending of circular plates of radius $r_1 = 1$ m. The plate thickness can be constant [$H(r) = H_* = \text{const}$] or variable: for a simply supported plate,

$$H(r, s) = sH_* + 2H_*(1-s)(r_1^2 - r^2)/r_1^2 \qquad (0 \leqslant r \leqslant r_1, \quad 0 < s \leqslant 1) \tag{27}$$

or

$$H(r, s) = sH_* + \frac{H_*\pi^2}{4(\pi - 2)}(1-s)\cos\left(\frac{\pi r}{2r_1}\right) \qquad (0 \leqslant r \leqslant r_1, \quad 0 < s \leqslant 1); \tag{28}$$

for a clamped plate,

$$H(r, s, r_{\min}) = sH_* + \frac{H_*(1-s)}{r_{\min}^4 - r_{\min}^2 r_1^2 + r_1^4/3}(r_{\min}^2 - r^2)^2 \qquad (0 < s \leqslant 1, \quad 0 < r_{\min} < r_1) \tag{29}$$

or

$$H(r, s, r_{\min}) = sH_* + \frac{H_*(1-s)\cos^2(\pi r/(2r_{\min}))}{1/2 + (r_{\min}/(\pi r_1))\sin(\pi r_1/r_{\min}) + (r_{\min}/(\pi r_1))^2(\cos(\pi r_1/r_{\min}) - 1)},$$

$$0 < r_{\min} < r_1, \qquad 0 < s \leqslant 1. \tag{30}$$

If the plate thickness is set in the form (27)–(30), its volume equals the volume of a plate of constant thickness H_*. It follows from Eqs. (27)–(30) that $dH/dr = 0$ ($r = 0$) at the plate center; for $0 < s < 1$, Eqs. (27) and (28) predict that the plate thickness at the edge $r = r_1$ is smaller than at the center ($r = 0$); the parameter $r_{\min}$ in (29) and (30) determines the polar radius r that ensures the minimum (if $0 < s < 1$) plate thickness $H(r_{\min}, s, r_{\min}) = sH_*$; for $s = 1$, Eqs. (27)–(30) predict that the plate has a constant thickness H_*.

The external distributed load is an explosive-type frontal load

$$p(r,t) = p(t) = \begin{cases} p_0 = \text{const} > 0, & 0 < t \leqslant T_0, \\ 0, & t > T_0 > 0 \end{cases} \tag{31}$$

or

$$p(r,t) = p(t) = p_0 \exp(-\alpha t) \qquad (t > 0), \tag{32}$$

where p_0 is the load intensity or the load at the initial time $t_0 = 0$ and $\alpha = 12$ sec^{-1} is the load attenuation parameter. (Again, another law of time variation of the explosive load can be prescribed [2]; this is not important for the present study.)

Below we consider plates made of the D16 aluminum alloy ($\rho = 2780$ kg/m^3 and $\sigma_s = 380$ MPa [15]) or of high-quality low-carbon steel ($\rho = 8000$ kg/m^3 and $\sigma_s = 248$ MPa [4]). The viscous hardening coefficient $E_s = 90.9$ MPa $\cdot$ sec for steel was obtained on the basis of tabular data from [4] by the least squares technique. In all calculations performed, we assumed that $E = 10^{16}$ Pa $\cdot$ sec [see Eq. (4)], which corresponds to the viscoplastic model approaching the model of a rigid-viscoplastic solid.

To test the method described in Sec. 2, we compare the results of numerical computations with the known analytical solution [1] obtained by an ideal rigid-plastic scheme ($E_s = 0$) for a simply supported plate of constant thickness H_* under dynamic loading (31). According to [1], two levels of loading have to be distinguished: 1) loading of low and medium intensity, which provides

$$p_s < p_0 \leqslant 2p_s; \tag{33}$$

2) loading of high intensity, which provides

$$p_0 > 2p_s. \tag{34}$$

In Eqs. (33) and (34),

$$p_s = 6M_s/r_1^2, \qquad M_s = \sigma_s H_*^2/4, \tag{35}$$

M_s is the ultimate moment, and p_s is the ultimate uniformly distributed transverse load.

At the loading level (33), no translationally moving plastic zones occur in the plate, the time T_f of motion termination (final time) is

$$T_f = p_0 T_0/p_s, \tag{36}$$

and the final flexure is calculated by the formula

$$w(r,T_f) = \frac{p_0(p_0 - p_s)}{\rho H_* p_s}\, T_0^2 \Big(1 - \frac{r}{r_1}\Big), \qquad 0 \leqslant r \leqslant r_1, \tag{37}$$

i.e., the mid-plane of the plate is deformed to a cone. At the loading level (34), plate motion is accompanied by the emergence of a translationally moving plastic circular zone, which decreases with time and shrinks to the plate center. The time of motion termination is again determined by Eq. (36), whereas the final flexure is calculated as

$$w(r,T_f) = \begin{cases} \dfrac{p_0 T_0^2}{2\rho H_*}\Big[\dfrac{p_0}{2p_s}\Big(3 - \dfrac{r}{r_1} - \dfrac{r^2}{r_1^2} - \dfrac{r^3}{r_1^3}\Big) - 1\Big], & 0 \leqslant r \leqslant r_p, \\ \dfrac{p_0 T_0^2}{2\rho H_*}\Big[\dfrac{p_0}{2p_s}\Big(3 - \dfrac{r_p}{r_1} - \dfrac{r_p^2}{r_1^2} - \dfrac{r_p^3}{r_1^3}\Big) - 1\Big]\Big(1 - \dfrac{r_p - r}{r_p - r_1}\Big), & r_p < r \leqslant r_1, \end{cases} \tag{38}$$

where the value of r_p is determined by the equation

$$\frac{p_0}{2p_s} = \frac{r_1^3}{(r_1 - r_p)^2(r_1 + r_p)}. \tag{39}$$

TABLE 1

Comparison of Analytical and Numerical Solutions of the Problem of Inelastic Dynamics of a Circular Plate Made of Low-Carbon Steel

Solution	$p_0 = 2p_s = 1.1904$ MPa		$p_0 = 4p_s = 2.3808$ MPa	
	T_f, sec	$W_{\max}$	T_f, sec	$W_{\max}$
Analytical	0.2	0.744	0.4	3.72
Numerical	0.193 (3.5%)	0.581 (22.0%)	0.388 (3.0%)	3.60 (3.14%)

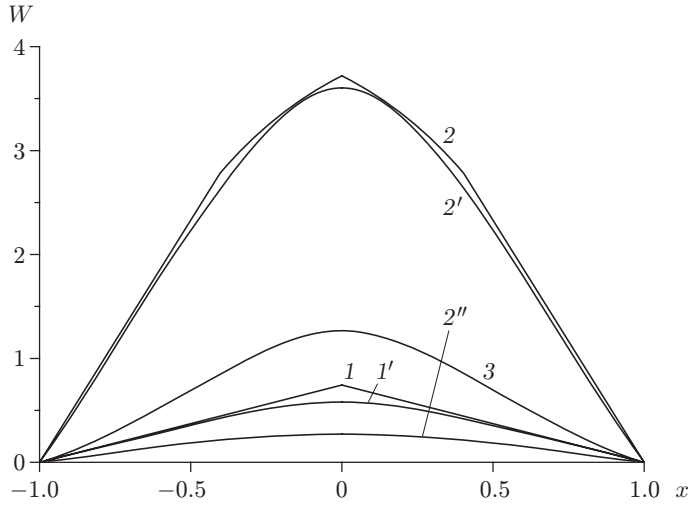

Fig. 1. Comparison of the final flexure of a circular plate determined analytically and numerically: calculation by Eq. (37) with $p_0 = 2p_s$ (1); numerical calculation with $p_0 = 2p_s$ (1′); calculation by Eqs. (38) and (39) with $p_0 = 4p_s$ (2); numerical calculation with $p_0 = 4p_s$ (2′); numerical calculation with $p_0 = 4p_s$ with allowance for viscous hardening (2″); numerical calculation for a clamped plate with $p_0 = 4p_s$ (3).

Table 1 contains the exact values calculated by Eqs. (36)–(39) and approximate values calculated by the scheme described in Sec. 2 for the time of motion termination T_f and the maximum dimensionless final flexure $W_{\max} = H_* w_{\max}/(2r_1^2)$, which arises at the plate center. In the calculations, the characteristic time period $T = 1$ sec used to study the plate motion was divided into 1000 layers ($\tau = T/1000$), and 201 nodes were set along the plate radius. The calculations were performed for medium-intensity loading ($p_0 = 1.1904$ MPa), which corresponds to $p_0 = 2p_s$ for a low-carbon steel plate of thickness $H_* = 0.04$ m, and for high-intensity loading ($p_0 = 2.3808$ MPa), which corresponds to $p_0 = 4p_s$ [see Eq. (35)]. The time of loading (31) was $T_0 = 0.1$ sec. The figures in parentheses in Table 1 show the difference in the numerical and analytical solutions expressed in percent.

Figure 1 shows the dimensionless final flexure $W(x) = H_* w(x)/(2r_1^2)$ ($x = r/r_1$) determined numerically and by Eqs. (37)–(39). (The maximum values of flexure on curves 1, 1′, 2, and 2′ are listed in Table 1.) It follows from Table 1 and Fig. 1 that the final time T_f obtained numerically is in good agreement with the value of T_f predicted by Eq. (36); instead, the final flexure calculated by the scheme described in Sec. 2 under low- and medium-intensity loading can differ from the analytical solution (37) by dozens of percent (cf. curves 1 and 1′), but this difference between the numerical solution and analytical solution (38), (39) under high-intensity loading rapidly decreases with increasing loading amplitude and reaches approximately 3% already at $p_0 = 4p_s$ (see Table 1 and curves 2 and 2′ in Fig. 1). With a further increase in loading intensity p_0, the error of the numerical solution remains roughly unchanged. Thus, for $p_0 = 8p_s = 4.7616$ MPa, the values of T_f and $W_{\max}$ obtained numerically and analytically differ by 2 and 3%, respectively.

It should be noted that the numerical solution obtained by the scheme described in Sec. 2 cannot unlimitedly approach the analytical solution (37)–(39). This is caused by three factors. First, the analytical solution (37)–(39) is obtained on the basis of an ideal rigid-plastic model, whereas the numerical solution is obtained on the basis of

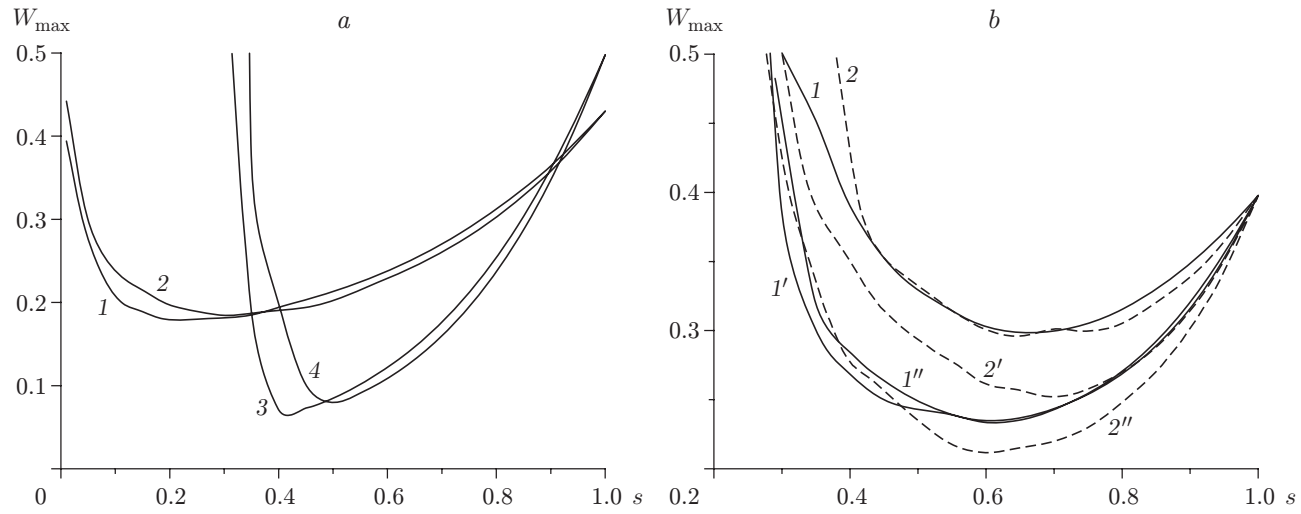

Fig. 2. Maximum final flexure of simply supported (a) and clamped (b) circular plates versus the contouring parameter: (a) curves 1 and 2 refer to the calculation by Eqs. (27) and (28) for steel plates, respectively, curves 3 and 4 refer to the calculation by Eqs. (27) and (28) for aluminum plates, respectively; (b) the solid and dashed curves show the calculations with the use of contours (29) and (30), respectively; $r_{\min} = 0.9r_1$ (1 and 2), $0.8r_1$ (1′ and 2′), and $0.7r_1$ (1″ and 2″).

a viscoplastic model (4) in which the solution depends on linear viscosity $E \neq \infty$ necessary to ensure unambiguity of the dependence $\sigma \sim \xi$. Second, the analytical solution is obtained with the Trask yield criterion [1], and the numerical solution is obtained with the Mises yield criterion [6]. Third, it follows from Eqs. (36)–(38) that the magnitude of the final flexure and the final time substantially depend on the excess pressure (on the value of $p_0/p_s > 1$) responsible for plate motion. If the loading intensity p_0 is fixed, the excess pressure is determined by the ultimate load p_s, which is calculated by Eq. (35) if the Trask yield criterion is used. If the Mises yield criterion is used, $p_s \approx 6.33M_s/r_1^2$ [16] [i.e., 5.5% greater than the value predicted by Eq. (35)], which leads to reduction of the excess pressure. These factors are responsible for reduction of the final time and the magnitude of the final flexure determined by the scheme described in Sec. 2, as compared with the analytical solution (36)–(39), especially for low- and medium-intensity loading. The analytically calculated final flexure (37)–(39) is known to exceed the experimental value by 30–80%; that is why the numerical solution agrees better with the experiment than the analytical solution [2].

The results listed in Table 1 are obtained by an ideal rigid-plastic model and a viscoplastic model ($E_s = 0$). If we take into account the dependence of the yield stress of low-carbon steel on the strain rate ($E_s \neq 0$), we obtain different values of the final time and final flexure. Thus, curve 2″ in Fig. 1 characterizes the final flexure of the plate with allowance for viscous hardening of its material at $p_0 = 4p_s$. A comparison of curves 2′ and 2″ shows that allowance for the dependence of the yield stress on the strain rate substantially reduces the maximum values of the final flexure (almost by a factor of 14), which agrees with experimental data [2].

In addition, the magnitude of the final flexure is significantly affected by the manner of plate attachment. Curve 3 in Fig. 1 characterizes the final flexure of a clamped plate under loading intensity $p_0 = 4p_s = 2.3808$ MPa without allowance for viscous hardening ($E_s = 0$). A comparison of curves 2′ and 3 shows that replacement of a simply supported plate by a clamped plate leads almost to a threefold decrease in the final flexure. Viscous hardening of steel being taken into account, the maximum final flexure is almost 30 times smaller than the maximum on curve 3.

Below we considered the dynamics of plates of constant thickness H_*. By varying the plate contour, we can control the final flexure whose values within the viscoplastic model characterize the degree of structural damage. Figure 2 shows the maximum final flexure $W_{\max}$ of simply supported (Fig. 2a) and clamped (Fig. 2b) plates versus the contouring parameter s in Eqs. (27)–(30) under explosive-type loading (32) of different intensities p_0. Curves 1 and 2 in Fig. 2a are calculated with the use of Eqs. (27) and (28), respectively, for steel plates with characteristic

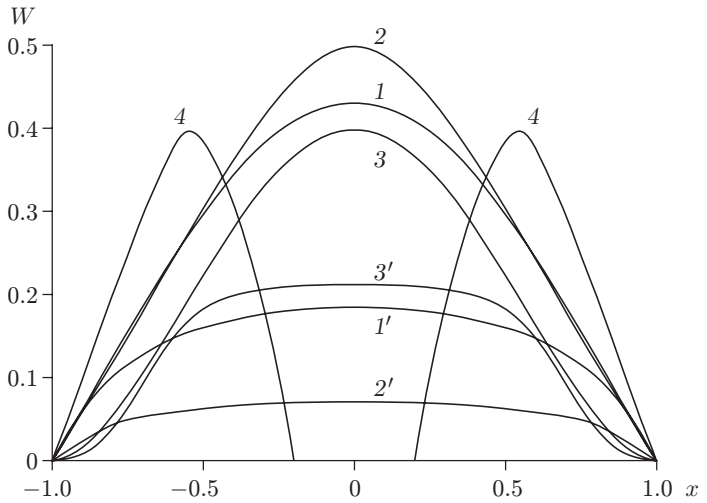

Fig. 3. Final flexure of circular and ring-shaped plates of constant and variable thickness with different types of attachment: simply supported steel plates with thickness distributed by Eq. (28) with $s = 1.0$ (1) and 0.3 (1′); simply supported aluminum plates with thickness distributed by Eq. (27) with $s = 1.0$ (2) and 0.4 (2′); clamped steel plates with thickness distributed by Eq. (29) with $r_{\min} = 0.7r_1$ and $s = 1.0$ (3) and 0.6 (3′); curve 4 refers to the simply supported ring-shaped aluminum plate of constant thickness.

sizes $H_* = 0.04$ m and $r_1 = 1$ m with allowance for viscous hardening of the material for an initial load $p_0 = 5$ MPa. Curves 3 and 4 are obtained with the use of Eqs. (27) and (28), respectively, for plates made of the D16 alloy, with the same characteristic sizes, for $p_0 = 1.8$ MPa (the yield stress of aluminum alloys is independent of the strain rate [17]). All curves in Fig. 2b are obtained for clamped steel plates with the same characteristic sizes for an initial load $p_0 = 15$ MPa. The solid and dashed curves are calculated by Eqs. (29) and (30), respectively, for different values of the parameter $r_{\min}$. Thus, curves 1 and 2 are obtained for $r_{\min} = 0.9r_1$ curves 1′ and 2′ are obtained for $r_{\min} = 0.8r_1$, and curves 1″ and 2″ are obtained for $r_{\min} = 0.7r_1$.

All curves in Fig. 2 have local minimums, and the values of $W_{\max}$ in these minimums is several times smaller than that at $s = 1$ (for constant-thickness plates). Therefore, rational selection of the plate thickness can ensure severalfold reduction of the final flexure. Figure 3 shows the final flexure $W(x)$ for some contoured (curves 1′–3′) and non-contoured (curves 1–3) plates.

Scheme (22)–(25) also allows calculating inelastic dynamics of ring-shaped plates. Curves 4 in Fig. 3 characterize the final flexure of a simply supported ring-shaped ($r_0 = 0.2r_1$) aluminum plate of constant thickness $H_* = 0.04$ m under initial loading $p_0 = 4.5$ MPa.

4. Conclusions. The method described in the present paper allows effective solution of problems of viscoplastic dynamics of plates of constant and variable thickness under explosive loading. Definition of a rational distribution of the plate thickness offers a severalfold decrease in the maximum final flexure and, hence, a significant decrease in plate damage with a fixed consumption of the plate material.

This work was supported by the Russian Foundation for Basic Research (Grant No. 05-01-00161-a).

REFERENCES

1. H. G. Hopkins and W. Prager, "On the dynamics of plastic circular plates," *Z. Angew. Math. Phys.*, **5**, No. 4, 317–330 (1954).
2. K. L. Komarov and Yu. V. Nemirovskii, *Dynamics of Rigid-Plastic Structural Elements* [in Russian], Nauka, Novosibirsk (1984).
3. M. I. Erkhov, *Theory of Ideal Plastic Solids and Structures* [in Russian], Nauka, Moscow (1978).
4. F. V. Warnock and J. A. Pope, "The change in mechanical properties of mild steel under repeated impact," in: *Appl. Mechanics Proceedings*, Vol. 157, Inst. of Mech. Eng. (1947).

5. P. M. Ogibalov, *Issues of Dynamics and Stability of Shells* [in Russian], Izd. Mosk. Univ., Moscow (1963).
6. L. M. Kachanov, *Foundations of the Theory of Plasticity*, North-Holland, Amsterdam–London (1971).
7. L. M. Kachanov, *Theory of Creep* [in Russian], Fizmatgiz, Moscow (1960).
8. Yu. V. Nemirovskii and A. P. Yankovskii, "Elastoplastic bending of rectangular plates reinforced by fibers with a constant cross section," *Mekh. Kompoz. Mater. Konstr.*, **41**, No. 1, 17–36 (2005).
9. V. V. Sokolovskii, *Plasticity Theory* [in Russian], Vysshaya Shkola, Moscow (1969).
10. Yu. V. Nemirovskii and A. P. Yankovskii, "Generalization of the Runge–Kutta methods and their application to integration of initial-boundary problems of mathematical physics," *Sib. Zh. Vychisl. Mat.*, **8**, No. 1, 51–76 (2005).
11. N. N. Malinin, *Applied Theory of Plasticity and Creep* [in Russian], Mashinostroenie, Moscow (1968).
12. V. Z. Vlasov and N. N. Leont'ev, *Beams, Plates, and Shells on an Elastic Base* [in Russian], Fizmatgiz, Moscow (1960).
13. N. N. Kalitkin, *Numerical Methods* [in Russian], Nauka, Moscow (1978).
14. A. A. Samarskii, *Theory of Difference Schemes* [in Russian], Nauka, Moscow (1989).
15. *Composite Materials: Handbook* [in Russian], Naukova Dumka, Kiev (1985).
16. H. G. Hopkins and W. Prager, "The load-carrying capacities of circular plates," *J. Mech. Phys. Solids*, **2**, No. 1, 1–13 (1953).
17. C. J. Maiden and S. J. Green, "Compressive strain rate tests on six selected materials at strain rate from 10^{-3} to 10^4 in/in/sec," *J. Appl. Mech.*, **33**, 496–504 (1966).